



**Acoustics'08
Paris**
June 29-July 4, 2008

www.acoustics08-paris.org

A contact solver suitable for tyre/road noise analysis

Arjan Schutte, Ysbrand Wijnant and André De Boer

University of Twente, Dept. Mechanical Engineering, P.O. Box 217, 7500 AE Enschede,
Netherlands

j.h.schutte@utwente.nl

Road traffic noise is a major environmental problem. The interaction between tyre and road surface, the major noise source, is highly non-linear and is therefore best described in the time domain. The currently used contact models used for tyre/road noise have problems with either accuracy or calculation speed. At the Structural Dynamics and Acoustics group of the University of Twente an alternative contact algorithm has been developed. One characteristic feature of this algorithm is that, while solving the set of equations, the contact condition, i.e. the condition stating that there is no contact between the bodies, is satisfied exactly. Hence, there is no need for contact elements or contact parameters. The major advantage of the new approach is the possibility to speed up the algorithm, using the multigrid method. In this paper the contact algorithm is applied to a two-dimensional finite element model. Coulomb friction is taken into account. Some test simulations illustrate the algorithm.

1 Introduction

In modern society, traffic noise has become an important issue for mental health. A significant contributor to this noise pollution is tyre/road noise, which is caused by the interaction between tyre and road surface. The noise generating mechanisms have been identified, although there is discussion on the relative importance of these mechanisms. From experiments, it is known that spectra of tyre/road noise display a peak in the range of 500–2000 Hz [8]. Hence, tyre/road noise is a high frequency problem.

In order to predict and reduce tyre/road noise, different mathematical and empirical noise predicting models have been developed during the last decades. The main similarity between the mathematical models is that they can be separated in a tyre vibration model and a sound radiation model. Sound radiation has been modelled analytically by equivalent sources and numerically, by use of (in)finite elements or boundary elements. The tyre vibration models range from analytical models, where the tyre vibrations are modelled by means of a ring [1], shell [9] or plate [5], to numerical models based on finite elements. The finite element-based models use approximations in circumferential direction by e.g. an implementation of the Arbitrary Lagrangian Eulerian approach [6, 2] or by the use of waveguide finite elements [7]. The influence of a realistic tread profile cannot be modelled because of these approximations. Therefore, a full three dimensional model of the tyre has to be made. The current tyre models in the finite element package Abaqus are advanced, i.e. it is possible to analyze treaded tyres. However, the calculation times are large, since the calculation of high frequencies requires a fine mesh.

The currently used contact models used for tyre/road noise have problems with either accuracy or calculation speed. At the Structural Dynamics and Acoustics group of the University of Twente an alternative contact algorithm has been developed. A characteristic feature of this algorithm is that, while solving the set of equations, the contact condition, i.e. the condition that there is no overlap between the bodies, is satisfied exactly. Hence, there is no need for contact elements, contact parameters, Lagrange multipliers, or regularization. The major advantage of the new approach is the possibility to use multigrid methods to speed up the algorithm. In the field of elasto-hydrodynamic lubrication, multigrid and multilevel techniques have been used extensively to solve contact problems fast [11, 12]. Moreover, the proposed contact algorithm is stable and robust.

The new contact algorithm has been successfully applied in a finite difference formulation, where the tyre was modelled as a flexible ring [13]. In this paper, the contact algorithm is applied in a finite element model. The numerical model and the contact algorithm are explained in the next section; numerical experiments are presented afterwards.

2 Numerical model

The tyre is modelled using a Lagrangian approach, which can easily be replaced by an updated Lagrangian approach in order to be able to apply large rotations and deformations in a more advanced model [10]. In this section the finite element model, the contact model and the contact algorithm are discussed.

2.1 Finite element model

The equation of motion reads

$$\nabla \cdot \boldsymbol{\sigma} + \mathbf{b} = \rho \ddot{\mathbf{u}}, \quad (1)$$

where $\boldsymbol{\sigma}$ is the symmetric Cauchy stress tensor, ρ the density, \mathbf{b} the body forces and $\ddot{\mathbf{u}}$ the acceleration. Constitutive equations are needed to couple the Cauchy stress tensor and the density to the kinematics of the deformation. After integration over an arbitrary volume V , introduction of weight functions \mathbf{w} and application of the divergence theorem of Gauss, the weak form of this equation is

$$\int_V \mathbf{w} \cdot \rho \ddot{\mathbf{u}} dV + \int_V \nabla \mathbf{w} : \boldsymbol{\sigma} dV = \int_V \mathbf{w} \cdot \mathbf{b} dV + \int_S \mathbf{w} \cdot \mathbf{t} dS, \quad (2)$$

where $\mathbf{t} = \boldsymbol{\sigma} \cdot \mathbf{n}$ is the traction vector, \mathbf{n} the outward unit normal vector and S the boundary surface. The equilibrium problem is now discretized by dividing the domain in a number of elements. For the contact algorithm it is preferable to use linear shape functions. Following the Galerkin approach, the weight functions are chosen equal to the shape functions. Then, the equation of motion can be written as a system of coupled, second order differential equations in time

$$\mathbf{M} \ddot{\mathbf{u}} + \mathbf{C} \dot{\mathbf{u}} + \mathbf{K} \mathbf{u} = \mathbf{f}_{\text{ext}}, \quad (3)$$

where \mathbf{M} is mass matrix, \mathbf{C} the damping matrix, \mathbf{K} the stiffness matrix, \mathbf{u} the nodal displacement vector, and $\mathbf{f}_{\text{ext}} = \mathbf{f}_t + \mathbf{f}_b$ the external force vector, the sum of the nodal body forces and nodal traction forces (see the

righthand side of Eq (2)). Eq (3) can be solved in time when sufficient boundary conditions are applied. The fact that a tyre cannot penetrate the road surface, is an example of a boundary condition for the tyre. This contact behaviour is described by the contact model in the next section.

2.2 Contact model

Contact for finite elements is frequently studied in literature. For an overview the reader is referred to e.g. [4]. The traction vector \mathbf{t} working on the surface can be split in a normal component \mathbf{t}_N and tangential component \mathbf{t}_T according to

$$\mathbf{t} = \boldsymbol{\sigma} \cdot \mathbf{n} = \mathbf{t}_N + \mathbf{t}_T = t_N \mathbf{n} + \mathbf{t}_T, \quad (4)$$

where \mathbf{n} is the outward unit normal vector. Note that the traction is part of the external load vector in Eq (3).

2.2.1 Contact condition

The contact condition is a constraint equation, specifying that the tyre cannot penetrate the road surface. Hence, a gap function, i.e. the distance between the tyre and the road, g can be defined according to

$$g \geq 0. \quad (5)$$

where g is the perpendicular distance between a node of the tyre and the contact surface. For nodes in contact $g = 0$. Moreover there is assumed to be no adhesion between the two surfaces in contact, i.e. the contact forces can only be negative

$$t_N = \mathbf{t} \cdot \mathbf{n} \leq 0, \quad (6)$$

where t_N is the normal component of the traction vector \mathbf{t} and \mathbf{n} denotes the outward unit normal vector.

2.2.2 Friction model

When the tyre is in contact with the road, the friction model determines whether the tyre sticks or slips. Coulomb's friction law states that the tangential traction is limited by the normal traction according to

$$|\mathbf{t}_T| \leq \mu |\mathbf{t}_N|, \quad (7)$$

where μ is the friction coefficient. Nodes that fulfill Eq (7), stick to the surface and when $\mathbf{t} \geq \mu \mathbf{t}_N$ slip occurs. For frictionless contact, $\mu = 0$.

The interaction between tyre and road surface is inherently non-linear, and has to be solved in the time domain. The time domain is discretized and the used contact algorithm describes how Eq (3) is solved for every time step.

2.2.3 Contact algorithm

In each time step, the contact algorithm uses relaxation to calculate an update for each node individually. The applied algorithm has some similarities with the one used by Wu & Du [14], where nodal displacements are used as well. The working of the contact algorithm can best be explained by the flowchart as given in Fig 1.

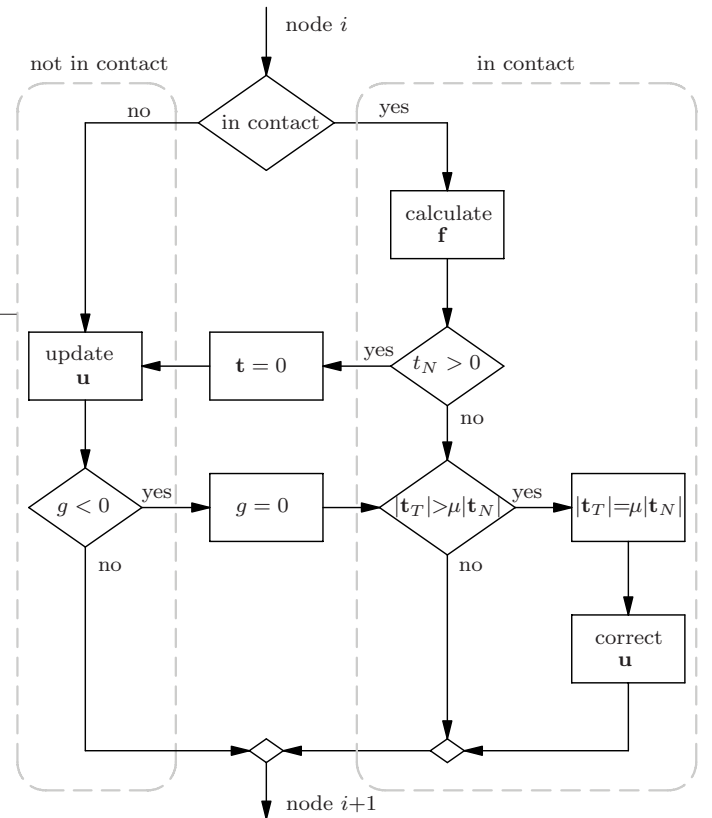


Figure 1: Flowchart of the contact algorithm.

For simplicity, the calculation steps in the algorithm are given for the static case. Consider an arbitrary node i , the algorithm first checks if the node is in contact. For nodes in contact a nodal force \mathbf{f}_i is calculated which is required to keep the node at that position, according to

$$\mathbf{f}_i = \mathbf{K}_i \mathbf{u}, \quad (8)$$

where \mathbf{K}_i is the rectangular nodal stiffness matrix. The length of \mathbf{f}_i equals the number of dimensions. The total external force consists of a body and traction component. The algorithm checks if the normal component of the traction t_N is negative. In case the traction t_N is positive (tensile), the node is released and the traction \mathbf{t} is set to zero; the node is out of contact. Note that this not necessarily means that \mathbf{f}_i is zero, since body forces can be present. The displacement of the nodes out of contact is updated using Gauss-Seidel relaxation

$$\hat{\mathbf{u}}_i = \tilde{\mathbf{u}}_i + \frac{1}{\det(\mathbf{K}_{ii})} (\mathbf{f}_i - \mathbf{K}_{ii} \tilde{\mathbf{u}}), \quad (9)$$

where $\hat{\mathbf{u}}_i$ is the updated displacement vector of node i , $\tilde{\mathbf{u}}_i$ the original displacement vector of node i , \mathbf{f}_i the nodal external force vector and \mathbf{K}_{ii} the square nodal stiffness matrix which is the nodal part of \mathbf{K}_i . When a node has been displaced to a point below the surface, the node is in contact and put back on the surface ($g = 0$). Nodes in contact are considered to stick on the surface *a priori*. In order to check this assumption the nodes in contact are subjected to Eq (7). If the tangential traction is too high, the friction force is maximal ($|\mathbf{t}_T| \leq \mu |\mathbf{t}_N|$). The node slips along the surface ($g = 0$) and the displacement is corrected. In the next step, node $i+1$ is considered and the process continues until convergence has reached for all nodes.

2.3 Time integration

In the previous section, the static case is considered. For dynamic simulations a discretation in the time domain is necessary. Under appropriate contact conditions, Eq (3) is solved in time by a Newmark integration scheme. This implicit second order scheme is commonly used in finite element calculations, because of its consistency, stability and accuracy. In a dynamic calculation the contact algorithm calculates an update for the displacement in the new time step (\mathbf{u}_{n+1}). The acceleration and the speed at step $n+1$ follow from the previous time step n as

$$\ddot{\mathbf{u}}_{n+1} = \frac{1}{\beta \Delta t^2} \left(\mathbf{u}_{n+1} - \mathbf{u}_n - \Delta t \dot{\mathbf{u}}_n \right) - \left(\frac{1}{2\beta} - 1 \right) \ddot{\mathbf{u}}_n, \quad (10)$$

$$\dot{\mathbf{u}}_{n+1} = \frac{\gamma}{\beta \Delta t} \left(\mathbf{u}_{n+1} - \mathbf{u}_n \right) - \left(\frac{\gamma}{\beta} - 1 \right) \dot{\mathbf{u}}_n - \Delta t \left(\frac{\gamma}{2\beta} - 1 \right) \ddot{\mathbf{u}}_n, \quad (11)$$

where Δt is the time step, $\gamma = \frac{1}{2}$ and $\beta = \frac{1}{4}$ for unconditional stability. After the substitution of these relations in Eq (3) and application of the initial conditions, $\ddot{\mathbf{u}}_{n+1}$ and $\dot{\mathbf{u}}_{n+1}$ can be solved for each time step.

3 Results

To illustrate the working of the contact algorithm, a two-dimensional finite element model is built. Two numerical experiments will be presented in this section, i.e. a Hertzian contact and a bouncing ring. In the examples linear elastic material behaviour is considered.

3.1 Hertzian contact

To test the accuracy of numerical contact a non-trivial test is required for which the analytical solution is available, such as a Hertzian contact [3]. The Hertzian contact formulas describe the contact pressure distribution between two cylinders (line contact) or between two spheres (point contact).

The contact pressure distribution between two cylinders is given by the following analytical description:

$$p = p_0 \sqrt{1 - \xi^2}, \quad (12)$$

where p_0 is the maximum pressure, $\xi = x/a$ the normalized coordinate, x the Cartesian coordinate along the contact, and a the semi-contact width. The maximum pressure is given by

$$p_0 = \sqrt{\frac{PE^*}{\pi R}}, \quad (13)$$

where P is the normal load per unit length, E^* the effective Young's modulus and R the effective radius. The semi-contact width is given by the relation

$$a = \sqrt{\frac{4PR}{\pi E^*}}. \quad (14)$$

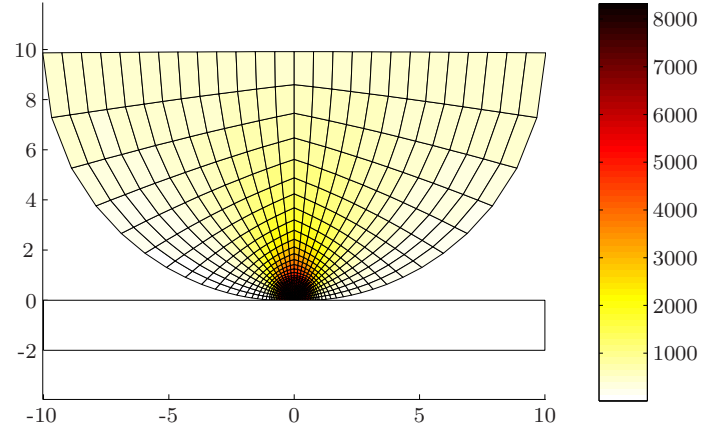


Figure 2: Stress distribution (N/mm) in the deformed mesh.

The effective Young's modulus is defined as

$$E^* \equiv \left(\frac{1 - \nu_1^2}{E_1} + \frac{1 - \nu_2^2}{E_2} \right)^{-1}, \quad (15)$$

where E_1 and E_2 denote the Young's moduli for the two cylinders and ν_1 and ν_2 the Poisson's ratios. The effective radius is defined as

$$R \equiv (1/R_1 + 1/R_2)^{-1}, \quad (16)$$

where R_1 and R_2 are the radii of the individual cylinders. For an elastic cylinder (1) on a flat rigid surface (2), Eqs (15) and (16) reduce to

$$E^* = \lim_{E_2 \rightarrow \infty} \left(\frac{1 - \nu_1^2}{E_1} + \frac{1 - \nu_2^2}{E_2} \right)^{-1} = \frac{E_1}{1 - \nu_1^2}, \quad (17)$$

$$R = \lim_{R_2 \rightarrow \infty} (1/R_1 + 1/R_2)^{-1} = R_1. \quad (18)$$

A numerical simulation is performed with the subsequent parameters: radius $R = 10$ mm, Young's modulus $E = 210 \cdot 10^3$ MPa, Poisson's ratio 0.3, a normal load per unit length $P = 1.0 \cdot 10^4$ N/mm. From Eqs (13) and (14) an analytical solution can be derived: maximum pressure $p_0 = 8571$ N/mm and semi-contact width $a = 0.7428$ mm.

The lower half of the cylinder is modelled with bilinear quadrilaterals and compressed on a rigid surface. The deformed mesh, together with the normal stress distribution, is given in Fig 2. The numerically and analytically derived contact pressure distribution is depicted in Fig 3. The numerical simulations show a good approximation of the Hertzian contact, with $p_0 = 8555$ N/mm and $0.73 < a < 0.80$ mm ($a = 0.75$ mm after interpolation). After mesh refinement, the numerical solution converges to the analytical solution. It can be concluded that the contact algorithm is able to predict normal contact pressures in frictionless contact correctly.

3.2 Bouncing ring

To validate the contact algorithm in dynamic cases, a fictive elastic ring is dropped on a rigid surface, as depicted in Fig 4. The ring has an outer radius of 0.5 m and an inner radius of 0.3 m. At the initial time step

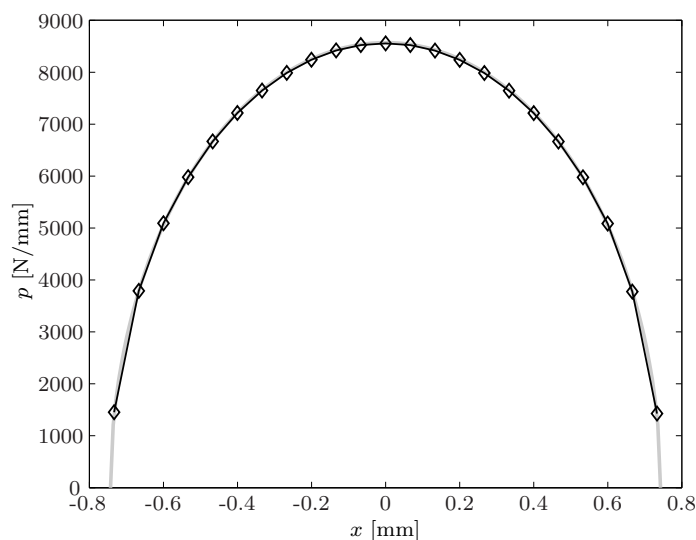


Figure 3: Pressure distribution (N/mm) in the contact patch, analytical (—) and numerical solution (\diamond).

($t = 0$ s), point A is located 0.2 m above the surface and the ring is at rest. The other parameters are chosen in accordance with a low eigenfrequency: Young's modulus $E = 200$ Pa, Poisson's ratio $\nu = 0.3$, the density $\rho = 1.0$ kg/m³, friction coefficient $\mu = 1.0$ and gravitational constant $g_0 = 9.81$ m/s². These settings result in a first eigenfrequency pair (bending mode) around 3.53 Hz. The time step ($\Delta t = 0.05$ s) is chosen to attenuate the high frequencies. In Fig 4 the first interaction between the ring and the surface is shown, which occurs between 0.2 and 0.21 s and satisfies the analytical solution (0.202 s). After 0.53 s the ring releases from the surface and will bounce again. Although the dynamic results look promising, experimental validation is needed and in progress.

4 Conclusions

The new contact algorithm, in which the contact condition is satisfied exactly, is applied in a two-dimensional finite element formulation. The algorithm is robust and stable and converges to the correct solution, without the use of contact elements or contact parameters. The major advantage of the new approach is the possibility to speed up the algorithm by using multigrid. The application of multigrid within the finite element formulation is necessary because of the large calculation times at high frequencies. The description of friction contact behaviour is validated by numerical simulations of a Hertzian contact. The application is not limited to static cases only, since the algorithm is successfully applied in a dynamic simulation. In the future, multigrid will be coupled to finite elements and anisotropic material behaviour will be added. The final goal is to compute the vibrations and radiated noise pattern of a profiled tyre rolling on a road.

Acknowledgements

The support of TNO and Vredestein within this CCAR project is gratefully acknowledged by the authors.

References

- [1] F. Böhm. *Mechanik des Gürtelreifens*. *Ingenieur Archiv*, 32(2):82–101, 1966.
- [2] M. Brinkmeier, U. Nackenhorst, and M. Zieffle. Finite element analysis of rolling tires – A state of the art review. In *Proceedings of International CTI Conference Automotive Tire Technology*, Stuttgart, Germany, 2007.
- [3] K.L. Johnson. *Contact Mechanics*. Cambridge University Press, UK, 1985.
- [4] G. Kloosterman. *Contact Methods in Finite Element Simulations*. PhD thesis, University of Twente, Enschede, The Netherlands, 2002.
- [5] W. Kropp. *Ein Modell zur Beschreibung des Rollgeräusches eines unprofilierten Gürtelreifens auf rauher Strassenoberfläche*. PhD thesis, Institut für Technische Akustik, Berlin, Germany, 1992.
- [6] U. Nackenhorst. The ALE-formulation of bodies in rolling contact – theoretical foundations and finite element approach. *Computer Methods in Applied Mechanics and Engineering*, 193:4299–4322, 2004.
- [7] C.-M. Nilsson. *Waveguide finite elements applied on a car tyre*. PhD thesis, Royal Institute of Technology, Stockholm, Sweden, 2004.
- [8] U. Sandberg and J.A. Ejsmont. *Tyre/Road Noise Reference Book*. INFORMEX, Harg, SE-59040 Kisa, Sweden, 2002.
- [9] W. Soedel. On the dynamic response of rolling tires according to thin shell approximations. *Journal of Sound and Vibration*, 41(2):233–246, 1975.
- [10] R.H.W. ten Thije. *Finite Element Simulations of Laminated Composite Forming Processes*. PhD thesis, University of Twente, Enschede, The Netherlands, 2007.
- [11] C.H. Venner. *Multilevel solvers for the EHL line and point contact problems*. PhD thesis, University of Twente, Enschede, The Netherlands, 1991.
- [12] Y.H. Wijnant. *Contact Dynamics in the field of Elastohydrodynamic Lubrication*. PhD thesis, University of Twente, Enschede, The Netherlands, 1998.
- [13] Y.H. Wijnant and A. de Boer. A new approach to model tyre/road contact. In *Proceedings of ISMA2006*, Leuven, Belgium, 2006.
- [14] B. Wu and X. Du. Finite element formulation of radial tires with variable constraint conditions. *Computers and Structures*, 55(5):871–875, 1995.

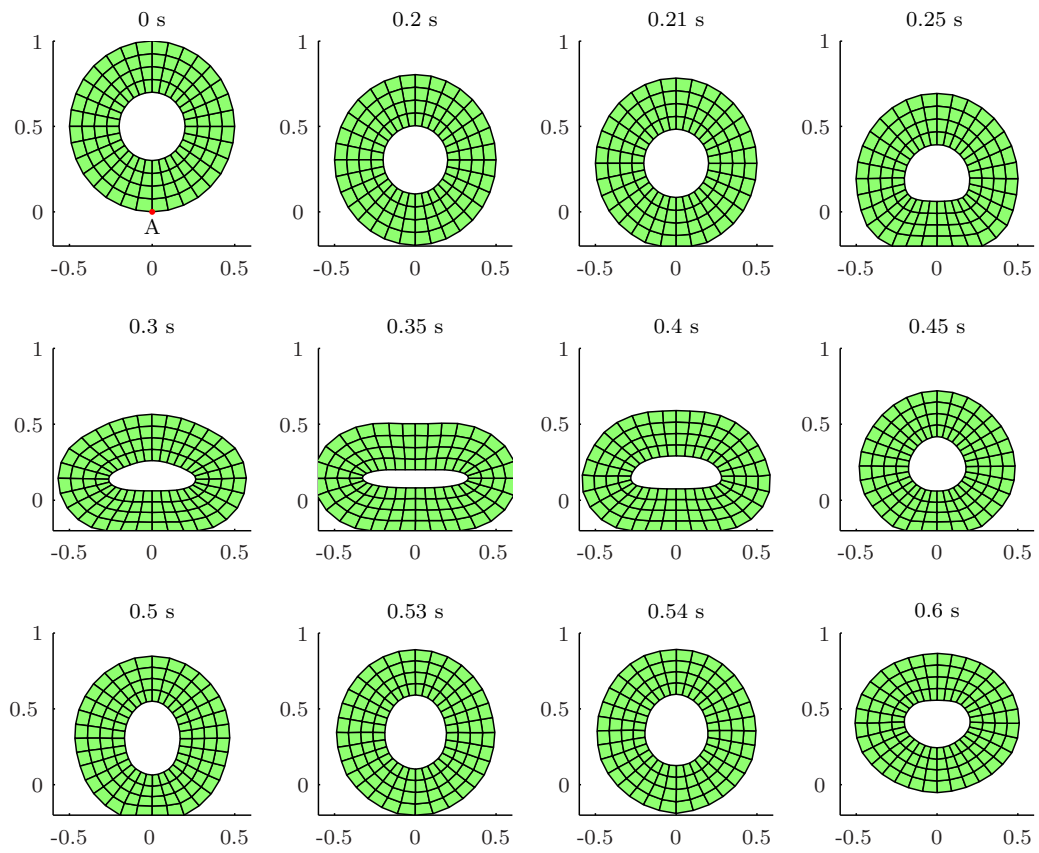


Figure 4: Bouncing ring on a rigid surface at different time steps